

# Goniometric Imaging of Paper Gloss

Tomi Kauppi<sup>1</sup>, Albert Sadovnikov<sup>1</sup>, Lasse Lensu<sup>1</sup>, Joni-Kristian Kamarainen<sup>1,2</sup>, Pertti Silfsten<sup>1</sup>  
and Heikki Kälviäinen<sup>1</sup>

<sup>1</sup>Machine Vision and Pattern Recognition Research Group  
Department of information Technology Lappeenranta University of Technology, Finland  
Firstname.Lastname@lut.fi

<sup>2</sup>Centre for Vision, Speech and Signal Processing, University of Surrey

## Abstract

*Gloss is a property of paper that is used to emphasize print quality and color appearance. However, standard gloss measuring devices are not able to provide sufficiently accurate information to reliably develop papers with specific gloss characteristics. In this paper, the behavior of gloss is studied using goniometric imaging and spectral color information. A goniometric imaging system is proposed to capture reflection images that reveal the spatial variation of the gloss over paper samples. The characteristics of the gloss are discussed by comparing the results of goniometric imaging, standard gloss measurements and spectroradiometric measurements.*

## 1 Introduction

The structure of paper is complex, and when combined with the process of papermaking, the production of paper of uniform quality is difficult. To meet the ever-increasing demands, research is needed in areas including raw materials, production technology, process control and end-products. To manage and improve the quality of paper and paper making, the quantitative and objective analysis of products and processes are needed. For this purpose, physically-measurable quantities can be used.

Gloss is an important property of paper that is desired in various printing purposes. It is a result of light interacting with paper and can be defined as physically-measurable quantity. The surface glossiness is declared either as a ratio of reflected light and reflection produced by an ideal mirror, or as the ratio of reflected light and the light emitted by the light source [4]. The perceptual and comprehensive abilities of human form the impression of gloss that cannot be accurately estimated by measuring a physical property. Gloss is used as one of the quality measures in the paper industry.

Standard test methods describe the gloss in one angle defining both the angle of incident light and the angle of measuring instrument with respect to the sample surface normal. The geometric configuration is chosen according to the material measured. The paper industry uses standardized 20° and 75° test method configurations for paper.

The measurement of hemispherical reflectance from the sample plane is proposed by many research groups, but it

is an exhaustive process and no simple method appears to be available [3, 2, 11, 1, 9, 6, 7, 5]. Research similar to this study is presented by Kimachi *et al.* [1]. The proposed measuring system suffered from problems making the optical axis of the camera and the centers of the two robot arms coincide, and therefore, a different approach for goniometric measurements is presented in this study.

The main contribution of this work is a goniometric imaging system for paper gloss measurements and preliminary tests to reveal the gloss characteristics. The system enables the generation of spatial gloss maps based on the goniometric measurements.

## 2 Goniometric imaging

In goniometric measurements it should be possible to place the measuring device and source of illumination on every hemisphere point over the sample surface. By changing the positions of the light and measuring device, the characteristics of gloss can be investigated.

The goniometer is the device that rotates the light source, sample plane and camera. To handle the goniometric movement, the goniometer is divided into three coordinate systems (frames) (Fig. 1). A frame defines relative pose (rotation and translation) of a coordinate system with respect to another coordinate system.

The basis of the goniometric system is the world frame, which is positioned at the center of the goniometer (Fig. 1). Movement of the camera and sample plane can be considered with respect to the world frame. The rotational movements of the goniometer are described in Fig. 2. Using these rotational movements, the position of the light source and the measuring device is made to correspond with the specific measuring configuration.

A specific measuring configuration is defined in the spherical coordinate system, where the illumination angle from the surface normal is  $(\theta_i)$  and the measurement direction is  $(\theta_r, \varphi_r)$ . A rotational movement of the goniometer in Fig. 2 is computed using the rotation matrices. The specific measuring configuration is first transformed into the cartesian coordinate system, where the light position is  $\mathbf{P}_l = (x_l, y_l, z_l)$  and the position of the camera is  $\mathbf{P}_c = (x_c, y_c, z_c)$  in Fig 3(a). The behavior of the goniometer can be defined from the initial position as

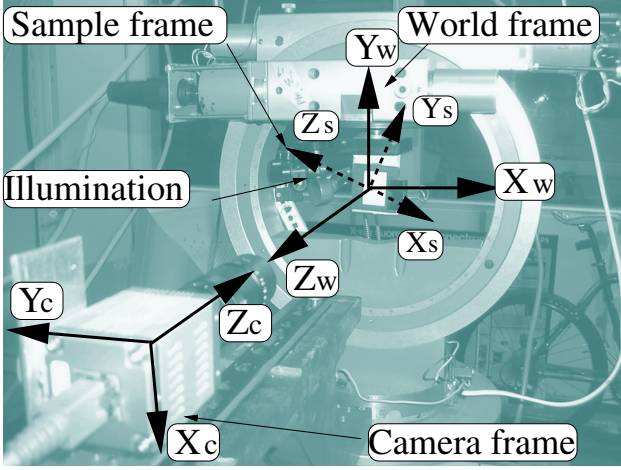


Figure 1: The coordinate systems. Light source is considered as a point in the coordinate systems.

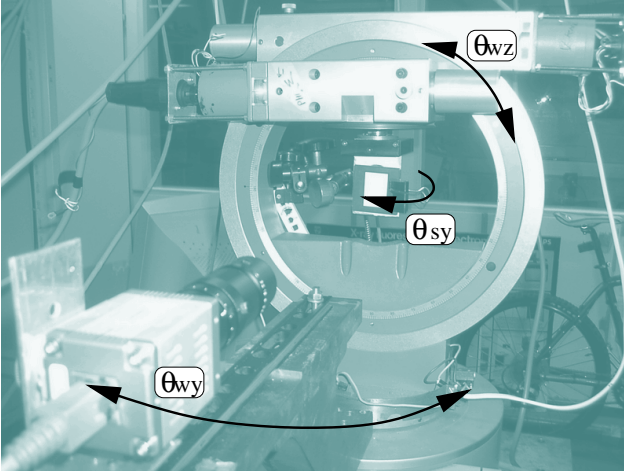


Figure 2: Possible rotational movements of goniometer.

$$\begin{aligned}
 {}^l\hat{\mathbf{P}} &= R_z(\theta_{wz}) {}^l\mathbf{P} \\
 {}^s\hat{\mathbf{P}} &= R_z(\theta_{wz}) R_y(\theta_{sy}) \mathbf{P}_s \\
 {}^c\hat{\mathbf{P}} &= R_y(\theta_{wy}) {}^c\mathbf{P}
 \end{aligned} \quad (1)$$

where  $R_y$  is the rotation around the y-axis,  $R_z$  is the rotation around the z-axis,  ${}^l\mathbf{P}$  is the initial position of light,  $\mathbf{P}_s$  is the initial coordinates of the four corner points,  ${}^c\mathbf{P}$  is the initial position of the camera.  ${}^l\hat{\mathbf{P}}$ ,  ${}^c\hat{\mathbf{P}}$  and  ${}^s\hat{\mathbf{P}}$  describe the orientation of the goniometer after rotating over the device angles  $(\theta_{sy}, \theta_{wz}, \theta_{wy})$ . Figs. 3(a) and 3(b) are the same in the sample frame, but in different orientation in the world frame. The mapping from the spesific configuration in Fig. 3(a) to Fig. 3(b) can be written as

$$\begin{aligned}
 {}^l\mathbf{P} &= R_z(\theta_{wz}) R_y(\theta_{sy}) \mathbf{P}_l \\
 {}^s\mathbf{P} &= R_z(\theta_{wz}) R_y(\theta_{sy}) \mathbf{P}_s \\
 {}^c\mathbf{P} &= R_z(\theta_{wz}) R_y(\theta_{sy}) \mathbf{P}_c.
 \end{aligned} \quad (2)$$

The problem in finding the correct pose for the goniometer, that corresponds to the spesific configuration, can be described as finding the device angles  $(\theta_{sy}, \theta_{wz}, \theta_{wy})$ , for which  ${}^l\hat{\mathbf{P}} = {}^l\mathbf{P}$  and  ${}^c\hat{\mathbf{P}} = {}^c\mathbf{P}$ . There can be more than

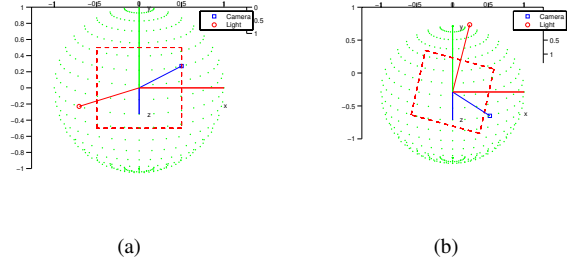


Figure 3: Orientations of the goniometer for solving the device angles: a) A spesific measuring configuration; b) An orientation of the goniometer that corresponds to the spesific measuring configuration;

one solution depending on the directions of the rotations, but a single correct solution can be found using the physical properties of the goniometer. The center of the goniometer for camera calibration can be extracted from the image using the rotation of sample plane around the z-axis. Depth calibration of the sample plane can also be extracted from the image by rotating the camera around the y-axis after calibrating the camera.

## 2.1 Compensating perspective effects

Homogeneous projective transformation of goniometric image compensates the perspective effects in the image and makes the measurement results comparable. By simulating the movement of the goniometer and camera with the device angles and intrinsic camera parameters, the orientation of the sample plane can be visualized. By knowing the orientation of the sample plane in image, the gloss images can be transformed to look as if they were all imaged from the direction of the surface normal to the center of the goniometer.

By finding the homogeneous projective transformation between image coordinates of sample after rotating goniometer and the image coordinates of sample in initial position, the rotated images can be mapped with projective transformations to the initial position. (Fig. 4). The image coordinates of the sample after rotating goniometer can be estimated from the known sample coordinates  ${}^s\mathbf{P}$  using perspective camera model [10]

$${}^{im}\mathbf{P} = K {}^c\mathbf{T}_s {}^s\mathbf{P} \quad (3)$$

where  ${}^{im}\mathbf{P}$  are the projective image coordinates of the sample,  ${}^c\mathbf{T}_s$  is mapping from the sample coordinate system to the camera coordinate system and  $K$  is the intrinsic camera parameters. The sample coordinates  ${}^s\mathbf{P}$  are acquired from the calibration. The image coordinates can be acquired by dividing each row of  ${}^{im}\mathbf{P}$  with the last row of  ${}^{im}\mathbf{P}$ .

The mapping from the sample frame to the camera frame can be conducted through the world frame

$${}^c\mathbf{T}_s = {}^c\mathbf{T}_w {}^w\mathbf{T}_s, \quad (4)$$

where  ${}^w\mathbf{T}_s$  is mapping from the sample frame to the world frame and  ${}^c\mathbf{T}_w$  is the mapping from the world frame to the camera frame. The mappings from camera and sample

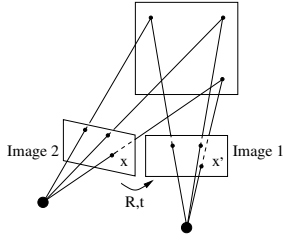


Figure 4: Projective transformation between two images. [8]

frames to the world frame can be derived from the goniometric behavior defined in Eq. 1 as follows:

$$\begin{aligned} wT_s &= \begin{pmatrix} R_{wz}R_{sy} & 0 \\ 0 & 1 \end{pmatrix} \\ wT_c &= \begin{pmatrix} R_{wy}^{ci}R & R_{wy}^{ci}P \\ 0 & 1 \end{pmatrix} \end{aligned} \quad (5)$$

where  $^{ci}P$  is the predefined initial position of the camera and  $^{ci}R$  the predefined initial orientation of the camera with respect to the world frame. The mapping from the world to the camera frame is a matrix inversion of camera to the world frame mapping  ${}^cT_w = wT_c^{-1}$ . Perspective compensated images in Fig. 5.

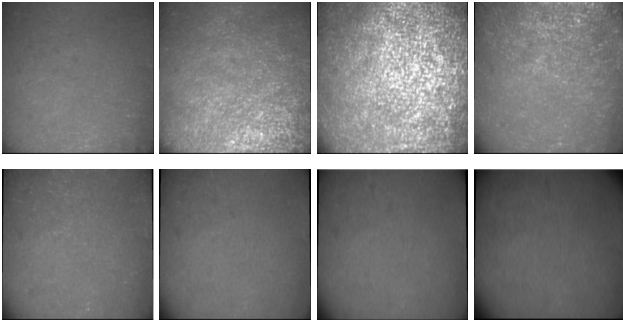


Figure 5: Images of paper 7 illuminated at  $20^\circ$  and measured in  $10^\circ$  steps from the angle  $0^\circ$  to angle  $70^\circ$ .

### 3 Results

A set of 9 different paper samples were chosen for preliminary tests with the TAPPI (Technical Association of the Pulp and Paper Industry) standard test method for specular gloss of paper and paper board at  $75^\circ$ , spectroradiometer and goniometric imaging system. The sample set consists of 5 different paper types and two of the paper types contained three samples of different basis weights. Paper b, Paper c and Paper d form one group and the rest of the samples belong to their own paper types. The same small area patches are used in all measurements. The standard specular measurements are shown in Table 1.

The standard measuring device gave an integrated value of gloss over the small area patch, but using the goniometric system it was possible to reveal the variation inside this small patch. The gloss images were taken with 12-bit

Table 1: Measurement results of TAPPI standard method for specular gloss and preliminary analysis of the goniometric imaging.

	$(\frac{g}{m^2})$	gloss value(TAPPI)	skewness	std
paper a	60	43, 2	0.1354	37.1882
paper b	48	49, 1	0.0723	30.4295
paper c	54	46, 4	-0.1987	32.1403
paper d	60	43, 1	-0.0986	38.3576
paper e	70	27, 9	-0.8823	31.9181
paper f	70	66, 4	1.364	44.561

b/w camera and the imaging resolution was  $1280 \times 1024$ . In Fig. 6 are illustrated the gloss of samples at standard illumination and measuring angle.

The intensity distributions of the gloss images in Fig. 7 reveal that glossy and non-glossy samples cause the intensity distributions to skew. The direction of the skewness indicates the shift from the 'average' glossiness to glossier or less glossier appearance. Skewness values calculated in Table 1 show the direction and magnitude of the shift. The standard deviation of the gloss image intensity values seem to correlate with the basis weight inside the same paper type (Table 1).

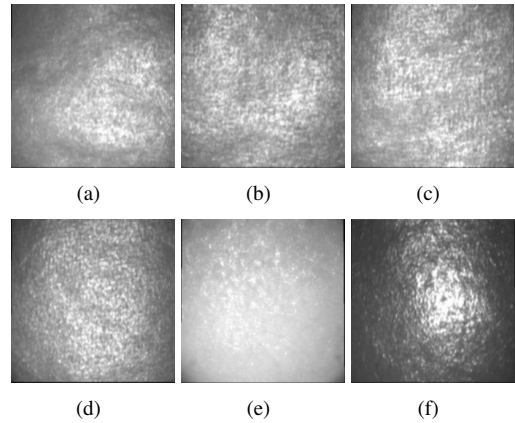


Figure 6: Images of all the 6 paper samples illuminated at  $20^\circ$  and measured from the specular angle.

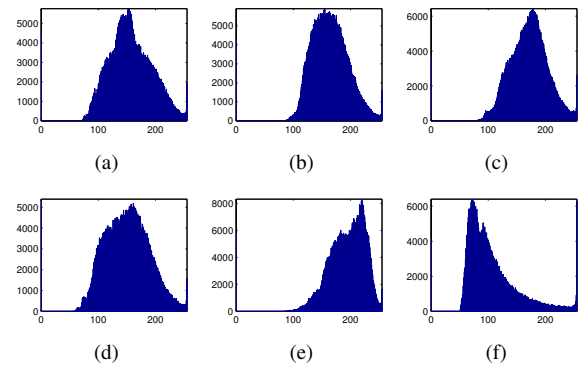


Figure 7: Intensity histograms of all the 6 paper samples illuminated at  $20^\circ$  and measured from the specular angle.

The color dependence of reflected light respect to measuring angle and illumination angle was studied within visible spectrum (380nm-780nm). The measurements were conducted with two illumination angles while varying measuring angle. The small changes in the shape of spectrum inside the same illumination configuration suggested that the color appearance was not dependent on the measuring angle, but on the illumination angle (Figs. 8 and 9). Since the reflected light spectrum was divided with the spectrum of illumination and the reflected energy at a  $75^\circ$  angle is evenly distributed between wavelengths, the reflected light has the same color as the illumination. However, the spectrum of  $20^\circ$  measurements differ from the measurements made at a  $75^\circ$ . Thus, the color of reflected light at a  $20^\circ$  angle is affected by the inner properties of paper and the light at a  $75^\circ$  angle is reflected from the surface. The goniometric gloss images seem to support the source of reflection. The result implies that the illumination angle determines which property of paper is measured.

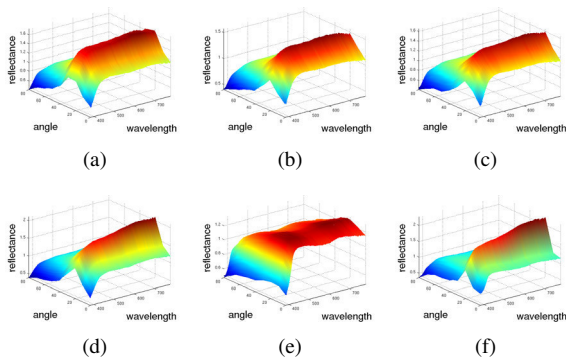


Figure 8: Measurements made with the spectroradiometer by illuminating the sample at  $20^\circ$  and measuring in  $10^\circ$  steps from angle of  $0^\circ$  to an angle of  $80^\circ$ .

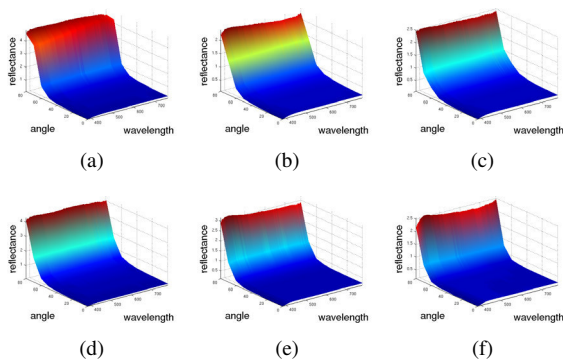


Figure 9: Measurements made with the spectroradiometer by illuminating the sample at  $75^\circ$  and measuring in  $10^\circ$  steps from an angle of  $5^\circ$  to an angle of  $75^\circ$  and an angle of  $0^\circ$ .

## 4 Discussion

An automated imaging goniometer was developed and limited tests related to its performance were performed. The current measuring system enables the measurement of gloss

maps that contain spatial information with the discrimination accuracy provided by the camera and optics. However, the image points of the measured gloss map do not share the same measuring configuration. In the future work, a set of measuring configurations will be used to obtain more accurate gloss information for the imaged points. In addition, a suitable target with known spatial gloss properties in goniometric measuring space is used to compensate for the nonideal effects caused by the imaging and illumination. High dynamic range imaging will also be experimented to minimize the loss of information caused by the insufficient dynamics of the camera at large angles with respect to sample plane normal. The goniometer will be used to study the minimum requirements for accurate gloss measurements, and the connection of gloss to perceivable unevenness of the surface.

## Acknowledgments

This work has been financially supported by European Union in the PAPVISION project (National Technology Agency of Finland Project No. 70049/03, 70056/04 and 40483/05) and Academy of Finland (Project 204708).

## References

- [1] M. T. A. Kimachi and S. Tominaga. A Goniophotometric System for Measuring the Object Surface Reflection using Robot Arms. In *Proceedings of the 9th IAPR conference on machine vision applications*, pages 47–50, Tsukuba Science City, Japan, 2005.
- [2] M.-C. Beland and J. M. Bennett. Effect of local microroughness on the gloss uniformity of printed paper surfaces. *Applied Optics*, 39(16):2719–2726, 2000.
- [3] H. H. J.S. Arney and P. Anderson. a Micro-Goniometer and the Measurement of Printed Gloss. *Journal of Imaging Science and Technology*, 48(5):458–463, 2004.
- [4] J.-E. Levlín and L. Sderbjelm. *Pulp and Paper Testing*. Papermaking Science and Technology. Fapet Oy, 1999. ISBN 952-5216-17-9.
- [5] M. Lindstrand. Gloss: measurement, characterization and visualization - in the light of visual evaluation. Licentiate Thesis, 2002. Linköping University, Sweden.
- [6] M. MacGregor and P.-. Johansson. Submillimeter gloss variations in coated paper; part 1. *Tappi Journal*, 73(12):161–168, 1990.
- [7] M. MacGregor and P.-. Johansson. Submillimeter gloss variations in coated paper; part 2. *Tappi Journal*, 74(1):187–194, 1991.
- [8] H. Richard and A. Zisserman. *Multiple View Geometry in Computer Vision*. Cambridge university press, 1998.
- [9] E. L. S.R. Marschner, S.H. Westin and K. E. Torrance. Image-Based Bidirectional Reflectance Distribution Function Measurement. *Applied Optics*, 39(16):2592–2600, 2000.
- [10] E. Trucco and A. Verri. *Introductory Techniques for 3-D Computer Vision*. Prentice-Hall, Inc, 1998. ISBN 0-13-261108-2.
- [11] K. J. Y. Kipman, P. Mehta and D. Wolin. A New Method of Measuring Gloss Mottle and Micro-Gloss using a Line-Scan CCD-Camera Based Imaging System. In *Proceedings of the NIP17: International Conference on Digital Printing Technologies*, pages 714–717, Fort Lauderdale, Florida, 2001.